ELSEVIER

Journal of Alloys and Compounds 293–295 (1999) 653–657

Journal of ALLOYS AND COMPOUNDS

A new electrode material for nickel–metal hydride batteries: MgNi–graphite composites prepared by ball-milling

Chiaki Iwakura*, Hiroshi Inoue, Shu G. Zhang, Shinji Nohara

Department of Applied Chemistry, College of Engineering, Osaka Prefecture University, 1-1 Gakuen-cho, Sakai, Osaka 599-8531, Japan

Abstract

MgNi–graphite composites prepared by ball-milling were found to show greatly enhanced charge–discharge characteristics with respect to the original MgNi alloy. There was an optimal ball-milling time for the preparation of the MgNi graphite composite with enhanced electrode performance, when the modification with graphite was limited to the surface layer of MgNi alloy. Raman and XPS investigations on the composites indicated a decline in the π-electron character of graphite and changes in the chemical states of the constituents on alloy surface, suggesting the possibility of charge transfer between graphite and MgNi alloy during ball-milling, which resulted in an increase in the surface Ni/Mg ratio.

Keywords: Nickel–metal hydride battery; MgNi alloy; MgNi–graphite composite; Raman; XPS

1. Introduction

Mg and Mg-based alloys have attracted increasing interest due to their extremely high capacity for hydrogen storage [1]. In general, however, they can only reversibly absorb and desorb hydrogen at high temperatures, say 250°C for Mg_2Ni, and at a higher temperature for metallic Mg at the atmospheric pressure [2].

Recently, Lei et al. [3] reported that amorphous MgNi alloy prepared by ball-milling of metallic Mg and Ni could charge and discharge hydrogen at room temperature. More recently, we found that a composite prepared by ball-milling of amorphous MgNi alloy with graphite exhibited much enhanced hydrogen-absorbing properties, for both the discharge capacity and the cycle life [4]. Kinetics measurements showed that the rate of hydrogen absorption for MgNi–graphite was much rapid than that of MgNi alloy [5]. It is of great interest and significance to evaluate the factors for such enhancement in the hydrogen-absorbing properties of MgNi–graphite composites.

In this study, we have carried out Raman and XPS together with electrochemical investigations on MgNi–graphite composites prepared by ball-milling, in order to elucidate the relation between their structural characteristics and hydrogen-absorbing properties.

2. Experimental

MgNi alloy was prepared by ball-milling a mixture of metallic Mg and Ni powders using a high energy ball-mill. To prepare the MgNi–graphite composite, MgNi alloy was first mixed with graphite powder of known weight in a mortar, then the mixture was ball-milled for a certain period of time. The detailed preparation procedures have been given elsewhere [4,5]. The prepared composites were kept in an Ar atmosphere with residual air pressure less than 10^{-2} torr, for the spectroscopic measurements or charge–discharge tests.

The preparation of negative electrode and the procedures for the charge discharge tests were also described elsewhere [5]. Raman spectra were recorded with a Renishaw Ramascope (system 2000) Raman spectrometer equipped with a HeNe laser (NEC). The wavelength of laser light was tuned to 632.8 nm, and the incident laser power at the samples was 30 mW. XPS spectra were measured with a PHI ESCA 5700 CI spectrometer using Mg Kα (1253.6 eV). The C1s peak of graphite or in some cases, the Ni2p of metallic Ni were used to calibrate peak positions. The quantitative data were obtained using a sensitive factor

*Corresponding author. Fax: +81-722-4-9283.
E-mail address: iwakura@chem.osakafu-u.ac.jp (C. Iwakura)

0925-8388/99/$ – see front matter
PII: S0925-8388(99)00360-6

method. The relative intensities of Ni2p and Mg2s peaks were used to estimate the ratio of Ni/Mg.

3. Results and discussion

The discharge capacities of the MgNi–graphite composite as a function of cycle number at different ball-milling time are shown in Fig. 1. Before ball-milling, the mixture of MgNi alloy and graphite showed a discharge capacity of ≈385 mA h g^{-1} at the first cycle, very close to that of MgNi alloy, ≈370 mA h g^{-1}. Upon ball-milling, the discharge capacity increased with ball-milling time until a maximum of ≈510 mA h g^{-1} was reached for the composite prepared by ball-milling the mixture for 10 min. When ball-milling the mixture for 20 min, the discharge capacity decreased again. Obviously, there is an optimal ball milling time, i.e. 10 min, for the preparation of the MgNi–20 wt.% graphite with high hydrogen absorbing performance. These results imply that ball milling is crucial for MgNi–graphite composite to exhibit an enhanced hydrogen absorbing property, which is not simply equal to that of MgNi plus that of graphite. Also, the enhancement is not due to the formation of crystalline $MgNi_3C_{0.75}$ after prolonged ball-milling. Some reactions between alloy and graphite under ball-milling are most likely to be the reasons. Furthermore, the possible contribution of graphite in the electric conductivity of the composite electrode during cycling was not important here. The same contribution in electrical conductivity could be expected even for the MgNi–graphite mixture, which did not show any enhancement in hydriding properties with respect to the initial MgNi alloy before ball-milling.

Shown in Fig. 2 are the Raman spectra observed for MgNi–graphite composites prepared by ball-milling with different content of graphite. A similar change in band intensities with the ball-milled graphite can be observed. The band at ≈1579 cm^{-1} clearly remained even after ball-milling, although with a decreased intensity, indicating

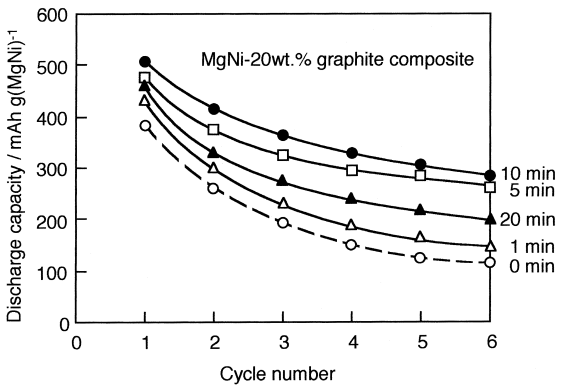

Fig. 1. The discharge capacity as a function of the cycle number for MgNi–20 wt.% graphite mixture ball-milled for different periods of time.

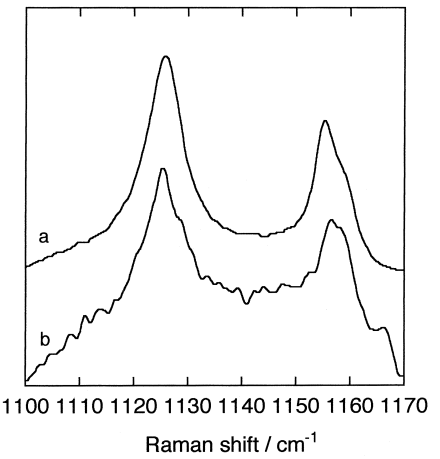

Fig. 2. Raman spectra observed for MgNi–x wt.% graphite composites. (a) $x=20$, (b) $x=2.0$.

that the graphite structure still exist in the MgNi–graphite composites. Besides the broadening and increase in intensity, no obvious changes in peak position can be observed for the band at 1326 cm^{-1}. The ratio of the relative band intensity at 1326 and 1579 cm^{-1}, $R=I_{1326}/I_{1579}$, correlated to the in-plane crystallite dimension L_a of graphite [6]. For the composites with various graphite content, this ratio did not vary substantially, indicating that the in-plane crystallite dimension L_a of graphite did not differ very much from sample to sample.

Another feature also seen from Fig. 2 is that a shoulder at ≈1602 cm^{-1} develops for the MgNi–graphite composites. While the content of graphite in MgNi–graphite composites is high, the shoulder is not so well distinguished due to the overlapping by 1579 cm^{-1} band. While the amount of graphite decreased, the shoulder can be easily distinguished, and both the E_{2g} band at around 1579 cm^{-1} and the shoulder at 1602 cm^{-1} show a tendency to shift to a higher wavenumber as the content of graphite decreases. In the ball-milling of graphite solely, neither this shoulder nor the peak shift can be observed, even after a prolonged milling time. Thus, it is likely that the above change in Raman spectra originates from the interaction of graphite with alloy during ball-milling.

For the same ball-milling time, lowering the content of graphite in MgNi–graphite composite leads to changes in graphite structure similarly to the change of the interior bands of graphite intercalation compounds (GICs) during the decrease of stage number, or an increase in intercalate content. It is well known that GICs show a Raman band different from that of graphite [7]. For the acceptor GICs, the interior E_{2g} band and the boundary E_{2g} band shifted to the high wavenumber as the intercalation stage decreased or, in other words, as the intercalate content increased [8]. On the other hand, the donor GICs shows a reverse tendency [9]. Such a tendency was due to the difference in nature of the charge-transfer reaction between the interca-

lates and the graphite layers which simultaneously influence the strength force correlated to the Raman modes. This is true also for the disordered carbon [10] and carbon nanotubes [11]. Thus, the interaction between graphite with MgNi alloy during ball-milling is a kind of charge-transfer in which graphite donates electrons to the alloy surface.

Fig. 3 shows the C1s XPS spectra of MgNi–20 wt.% graphite before and after ball-milling. Besides the minor changes in the symmetry, no other obvious change for the C1s peak at 284.6 eV can be observed. This result clearly shows that no carbide is formed in the present composites. Moreover, an obvious change is found in the binding energy region around 291.0 eV. The broad energy-loss feature at this region, which is about 6.4 eV higher than the C1s band, can be assigned to the interband transition involving a π-state excited by photoemitted electrons [12]. After ball-milling, a significant decrease in the relative intensity of this broad band was observed, clearly revealing that change in the electron state of graphite has occurred during ball-milling with MgNi alloy and the π-electron characteristic has significantly declined. Thus, together with the above Raman results, the present XPS data suggest that graphite reacted with alloy under high-energy ball-milling, a decline in the π-electron character of graphite or the disordered graphite has occurred, which indicated that graphite probably donated electron to the alloy surface during ball-milling.

In order to further probe the reaction of MgNi alloy with graphite, the MgNi alloys in MgNi–graphite composites were further studied in detail with XPS measurements. Fig. 4 shows the Mg2s XPS spectra observed with MgNi–20 wt.% graphite mixture before and after ball-milling. The Mg2s peaks at 90.0 eV before ball-milling, indicating that Mg exists as MgO on the MgNi alloy surface [13]. After ball-milling the peak shifted to a lower binding energy of 89.3 eV. The former can be attributed to the Mg oxide and

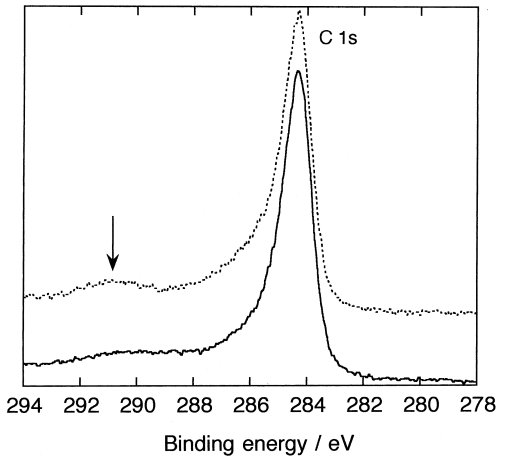

Fig. 3. The C1s spectra observed for the MgNi–20 wt.% graphite mixture before (dotted line) and after (solid line) ball-milling.

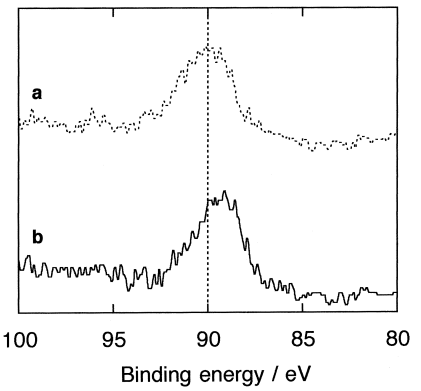

Fig. 4. The Mg2s XPS spectra observed for MgNi–20 wt.% graphite mixture before (a) and after (b) ball-milling.

the latter to the Mg which has a larger electron density than the original MgO existing on the alloy surface. This result indicated that the electron density around Mg had increased after ball-milling the MgNi alloy with graphite.

As shown above, the enhanced electrode performance of the MgNi composite can only be observed for the composites prepared after a relatively short ball-milling time, such as 10 min. Further ball-milling of the MgNi–graphite lead to the formation of a crystalline phase $MgNi_3C_{0.75}$, which may be due to the dissolution of carbon fragments into the alloy bulk. Thus, only the surface reaction of the MgNi alloy with the graphite is responsible for the improvement in electrode performance.

A previous study on the surface of the MgNi alloy has indicated that on the MgNi alloy surface, Mg exists as MgO and Ni as the metallic state [14]. Therefore, the reaction of the MgNi alloy surface with graphite under ball-milling should be mainly the reaction of MgO–Ni on the alloy surface with graphite. The electrons donated from graphite during ball-milling can therefore be considered to be trapped by MgO–Ni on the alloy surface. The increase in the electron density around Mg of MgO–Ni on the alloy surface, as indicated by the band shift of Mg2s to lower binding energy, can therefore be assigned to such an electron-trapping on the alloy surface.

Fig. 5 shows the $Ni2p_{1/2}$ and $Ni2p_{3/2}$ peaks for the MgNi alloy and MgNi graphite composites. For MgNi alloy, besides the $Ni2p_{3/2}$ peak at 852.4 eV, no other obvious peaks can be observed; while for the MgNi–graphite composites prepared by ball-milling, $Ni2p_{3/2}$ peaks appear not only at 852.4 eV, but also at a higher energy region. The $Ni2p_{3/2}$ peak at $\approx$852.4 eV can be assigned to the metallic Ni, while those at the high energy region are related the Ni oxides [15]. Thus, the above XPS data indicated that in MgNi–graphite composites, besides metallic Ni, nickel oxide also exist in part. It can also be clearly seen that the peak due to Ni^{2+} increased markedly in intensity with the increase in the amount of graphite in the composites. Since the exposure histories of the samples

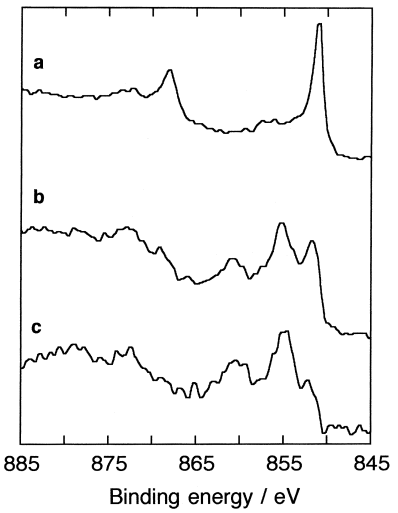

Fig. 5. The change of the Ni2p XPS spectra with graphite content for MgNi–x wt.% graphite composites. (a) $x=0$, (b) $x=1.0$, (c) $x=20$.

to air were all strictly controlled, this difference is considered to be mainly caused by graphite.

According to the results obtained for the MgNi alloys, Mg exists on the surface as an oxide while the Ni exists in the metallic state. Even after being exposed to air for a period of time, the amount of metallic Ni does not change significantly. These may suggest that Mg has the effect of preventing metallic Ni from being oxidized. Pure metallic Ni powder is, in contrast, usually oxidized to a significant extent under air exposure. These results indicate that by ball-milling MgNi alloy with graphite, the Ni in MgNi alloy becomes more isolated in the resultant composite than that in the initial MgNi alloy, and is therefore easily oxidized into NiO.

The surface Ni/Mg ratio of MgNi–graphite composites estimated from the XPS results was plotted against the graphite content in Fig. 6. It can be seen that by adding graphite, the composition of the surface layer of the MgNi alloy is modified significantly.

For MgNi alloy only, the Ni/Mg is only about 0.18 in the surface layer. While for the MgNi–graphite composite, containing 20 wt.% of graphite, the Ni/Mg increased to about 0.24. The low content of Ni on the MgNi alloy surface is due to the easy oxidative segregation of Mg onto the alloy surface. The change in Ni/Mg ratio for MgNi–graphite under ball-milling could be a direct reflection of the modified interaction of graphite on MgNi alloy, i.e. either the oxidation of Mg has been partially suppressed or the oxidation of Ni has been promoted. More importantly, the increased Ni/Mg ratio may contribute directly to the enhanced kinetics in hydrogen absorption for MgNi–graphite composite. A more significant amount of Ni can be detected for the composite samples sputtered with an Ar^+ beam which removed part of the graphite on the surface.

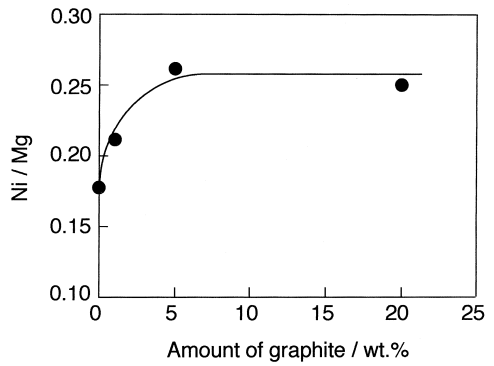

Fig. 6. The atomic ratio of Ni/Mg as a function of graphite content in MgNi graphite composites.

Based on the XPS and Raman results obtained above, the reaction of MgNi alloy with graphite under ball-milling may be proposed as follows:

Before ball-milling:

$$\text{Mg–Ni} + \text{residual } O_2 \rightarrow \text{Mg–O} \ldots \text{Ni} \quad (1)$$

Upon ball-milling:

$$\text{Mg–O} \ldots \text{Ni} + \text{Graphite} \rightarrow \text{Graphite} \ldots \text{Mg} \ldots \text{O–Ni} \quad (2)$$

The driving force for this change may be the reaction of the π-electron of graphite with the Mg . . . O groups on the alloy surface under high energy ball-milling. It is known that graphite can serve as a π-ligand [16]. The electron trapped on the alloy surface changed the chemical states of both Mg and Ni. The graphite–Mg units on the surface of the MgNi–graphite composite are expected to play a better role than MgO in the hydrogen absorbing process, as reported by Imamura et al. [17], that Mg–graphite could absorb hydrogen more effectively than metallic Mg.

Also, such a process closely resembles a partial reduction effect on Mg–O parts, and in the mean time, the Ni becomes more isolated and easily oxidized by residual oxygen or the oxygen in air. Thus, the reaction scheme can offer good evidence for the increase of the Ni/Mg ratio on the surface of the MgNi–graphite composite, which may be an important factor for the enhanced hydriding properties of MgNi–graphite composite.

4. Conclusions

In summary, we have demonstrated that an optimal ball-milling time exists for the preparation of MgNi–graphite composite with high electrode performance. The modification of graphite on the MgNi alloy in the MgNi–graphite composite is mainly a surface one. Raman and XPS investigations indicated the interaction of graphite with MgNi alloy occurred at the Mg part in the alloy. Such a reaction leads to the redistribution of electrons between Mg and Ni, which make the Ni more isolated from the

original alloy. Therefore, Ni can be oxidized more easily, and subsequently segregates more readily to the surface, resulting in the increase in Ni/Mg ratios for the MgNi–graphite composites. The enhanced ability of MgNi–graphite in hydrogen absorption is due to such interaction and the increase in the amount of isolated Ni on the surface.

Acknowledgements

This work has been supported in part by a Grant-in-Aid for Scientific Research on Priority Areas A of 'New Protium Function' no. 10148102, Grant-in-Aid for Scientific Research on Priority Areas A of 'Electrochemistry of Ordered Interfaces' no. 10131260, Grant-in-Aid for Scientific Research (B) no. 09555273, from the Ministry of Education, Science, Sports and Culture of Japan.

References

[1] J.J. Reilly, R.H. Wiswall, Inorg. Chem. 6 (1967) 2220.
[2] J.F. Stampfer, C.E. Holley, F.F. Suttle, J. Am. Chem. Soc. 82 (1960) 3504.
[3] Y.Q. Lei, Y.M. Wu, Q.M. Wang, J. Wu, Q.D. Wang, Z. Phys. Chem. 181 (1993) 379.
[4] C. Iwakura, S. Nohara, H. Inoue, Y. Fukumoto, Chem. Commun. (1996) 1831.
[5] S. Nohara, H. Inoue, Y. Fukumoto, C. Iwakura, J. Alloys Comp. 252 (1997) 16.
[6] F. Tuinstra, J.L. Koenic, J. Chem. Phys. 53 (1970) 1126.
[7] N. Caswell, S.A. Solin, Solid State Commun. 27 (1978) 961.
[8] M.S. Dresselhaus, G. Dresselhaus, Adv. Phys. 30 (1981) 139.
[9] H. Slig, L.B. Ebert, Adv. Inorg. Radiochem. 23 (1980) 281.
[10] M. Inaba, H. Yoshida, Z. Ogumi, J. Electrochem. Soc. 143 (1995) 2572.
[11] A.M. Rao, P.C. Eklund, S. Bandow, A. Thess, R.E. Smalley, Nature 388 (1997) 257.
[12] C.R.N. Rao, A. Govindaraj, B.C. Satishkumar, Chem. Commun. (1996) 1526.
[13] C.D. Wagner, P. Biloen, Surf. Sci. 35 (1973) 82.
[14] S.G. Zhang, K. Yorimitsu, T. Morikawa, S. Nohara, H. Inoue, C. Iwakura, J. Alloys Comp. 270 (1998) 123.
[15] F. Meri, L. Schlapbach, J. Less-Common Metals 172 (1991) 1252.
[16] M.E. Vol'pin, Yu.N. Novikov, N.D. Lapkina, V.I. Kasatochkin, Yu.T. Struchkov, M.E. Kazakov, R.A. Stukan, V.A. Povitskij, Yu.S. Karimov, A.V. Zvarikina, J. Am. Chem. Soc. 97 (1975) 3366.
[17] H. Imamura, N. Sakasai, Y. Kajii, J. Alloys Comp. 232 (1996) 218.